Wei *et al.*
Chinese Journal of Mechanical Engineering (2022) 35:101
https://doi.org/10.1186/s10033-022-00770-9

Chinese Journal of Mechanical Engineering

ORIGINAL ARTICLE

Open Access

Research on Surface Roughness of Supersonic Vibration Auxiliary Side Milling for Titanium Alloy

Xuetao Wei[1], Caixu Yue[1*], Desheng Hu[1], Xianli Liu[1], Yunpeng Ding[2] and Steven Y. Liang[3]

Abstract

The processed surface contour shape is extracted with the finite element simulation software. The difference value of contour shape change is used as the parameters of balancing surface roughness to construct finite element model of supersonic vibration milling in cutting stability domain. The surface roughness trial scheme is designed in the orthogonal test design method to analyze the surface roughness test result in the response surface methodology. The surface roughness prediction model is established and optimized. Finally, the surface roughness finite element simulation prediction model is verified by experiments. The research results show that, compared with the experiment results, the error range of the finite element simulation model is 27.5%–30.9%, and the error range of the empirical model obtained by the response surface method is between 4.4% and 12.3%. So, the model in this paper is accurate and will provide the theoretical basis for the optimization study of the auxiliary milling process of supersonic vibration.

Keywords: Side milling, Axial vibration, Ultrasonic milling, Finite element simulation, Linear regression, Surface roughness

1 Introduction

Nowadays, milling is deemed as one of the most commonly-used processing technologies in the manufacturing era. Milling is mainly used to process mold and other free-form surface parts. However, new materials such as high-strength aerospace alloy, etc., confront the following issues in milling: high cutting force, poor surface roughness, and rapid cutter abrasion. To achieve high precision and improve the service life of cutter and material removal rate, scholars around the world constantly explore new technology. Ultrasonic milling technology has been developed for many years, in which the supersonic vibration auxiliary milling is a kind of emerging unique milling technology. Compared with laser or electrical discharge milling, ultrasonic milling is more environmental-friendly. With the research breakthrough of scholars, the supersonic vibration milling has also obtained excellent progress in the actual application processing field. Currently, supersonic vibration milling with an ideal processing effect. It is generally applied in materials which are difficultly to process.

Biermann et al. [1] adopted the ultrasonic milling processing technology in the research on the milling of the thin-walled workpieces. They analyzed the research results to work out the influence rules and forming reason of vibration milling to workpiece surface roughness. Wang et al. [2] carried out the verification experiment of supersonic vibration auxiliary milling for optical glass K9, which concluded that the subsurface damage of materials is proportional to the change of cutting force and verified the accuracy of the prediction model. Shen et al. [3] established the tool trace model based on the transformation of tool trace characteristics after supersonic vibration, deeply analyzed the relationship between the tool trace and the workpiece's

*Correspondence: yuecaixu@hrbust.edu.cn

[1] Key Laboratory of Advanced Manufacturing and Intelligent Technology, Ministry of Education, Harbin 150080, China
Full list of author information is available at the end of the article

surface quality from the theoretical perspective. Finally, through experimental verification concluded that the workpiece's surface quality is related to the ratio between ultrasonic frequency and rotation speed of the main shaft, the larger the ratio is, the better the surface quality will be.

In recent years, with the gradual development of the finite element method, finite element analysis has been widely used in the field of cutting. The dynamic constitutive model [4–6], residual stress of thin-walled parts, prediction precision machining and micro-cutting of finite element technology, etc., are researched a lot, with remarkable achievements [7–10]. Moaz et al. [11] analyzed the influence of feed speed on surface roughness through the finite element simulation in the research on titanium alloy cutting, and concluded that the milling force is consistent with the surface roughness at different feed speeds; Thepsonthi [12] applied the finite element simulation method and utilized the finite element analysis method in the research on cutter abrasion condition in titanium alloy milling process; Muhammed et al. [13] established the finite element simulation model of 3D ultrasonic milling and traditional milling, and expounded the change of cutting force based on two kinds of processing technologies, and concluded that the vibration milling force reduces due to the increase of actual cutting speed and the continuous cutting of cutter; Sandipl et al. [14] conducted the modeling of 2D simulation model in the auxiliary processing process of rotary supersonic vibration, and in comparison to the traditional milling, concluded that the vibration milling process obviously improves the thermal softening effect of materials and the reduction of strength in clipping region based on finite element simulation of simulation model. Many research results [15, 16] indicate that the finite element analysis was advanced and efficient in the vibration cutting processing field and was deemed as one of the effective and necessary analysis and prediction methods. Finite element simulation analysis can optimize the processing technology parameters and simplify the experiment, especially playing an essential role in guiding the study of the coupling role among multi-factor parameters and the experimental result.

The application of the finite element simulation method in analysis of supersonic vibration auxiliary milling mainly focuses on the milling force and residual stress, and there is rare research on surface roughness of workpiece obtained through the supersonic vibration auxiliary milling processing in the finite element method. The 3D finite element simulation model of axial supersonic vibration auxiliary cutting titanium alloy is established to analyze the influence on processing surface quality after vibration.

2 Analysis of Finite Element Simulation for Surface Roughness

2.1 Interrupted Cutting Phenomenon Generated by Axial Supersonic Vibration

Since the flat milling cutter's side edge and blade helical angle mainly exert the axial supersonic vibration, in the axial vibration, the cutter and workpiece generate the relative radial motion, as shown in Figure 1. The analysis results regarding the relationship between actual cutting speed and indirect cutting show that the cutter and workpiece have intermittent contact in axial supersonic vibration milling. The milling cutter is deemed as single blade milling for the convenience of research [17].

Based on Eq. (1), the cutter's axial vibration velocity V_Z and time t have the following relationship:

$$V_Z = 2\pi Af \cdot \cos\left(2\pi ft\right), \tag{1}$$

where A and f refer to the vibration amplitude and vibration frequency, respectively.

The milling processing is defaulted at stable cutting status, and the main shaft is deemed to have uniform circular motion. So, the cutting speed V_c equation of the milling cutter is:

$$V_c = \pi dn/1000, \tag{2}$$

where d and n refer to the cutter diameter and rotation speed of the main shaft, respectively.

Then, the X-Y coordinate system is established in Figure 1. The coordinate axis x is found in the direction of the cutting edge, and the coordinate axis y perpendicular to the cutting edge is established. The cutting speed V_c and cutter's axial vibration speed V_z are decomposed in a new coordinate system. The rate in the direction of y can be transformed as:

$$V_y = V_c \cos\beta + V_z \sin\beta, \tag{3}$$

where β is the helix angle.

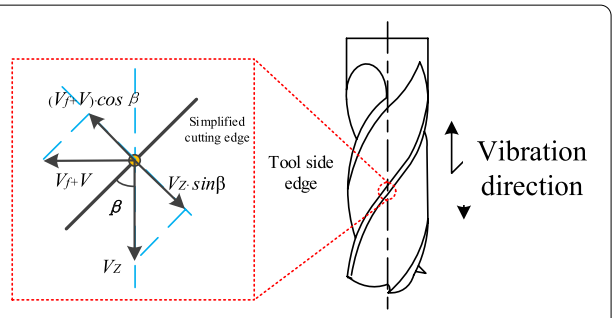

Figure 1 Relation drawings of separation speed for cutter workpiece

Due to the cutting tool moves up and down, the component velocity of V_z in the direction of y changes. When the $V_c\cos\beta$ and $V_z\sin\beta$ have the same direction, and the resultant speed in y direction constantly increases to the maximum value, the cutter is at the impact state. To expound the impact condition of supersonic vibration more intuitively, the acceleration coefficient G is introduced.

$$G = (V_z \sin\beta)' = -(2\pi Af)^2 \cdot \sin(2\pi Af) \cdot \sin\beta. \quad (4)$$

In combination with the above analysis results, the cutter has the following shock cutting conditions in the ultrasonic milling processing based on the theoretical analysis: ① The cutting tool is at the shock milling state when $G > 0$; ② The cutting tool is at the critical value of shock milling when $G = 0$; ③ The cutting tool is at the non-impact milling state when $G < 0$.

When $V_c\cos\beta$ and $V_z\sin\beta$ have the opposite direction, the resultant velocity direction will point to the path with a larger value, and the cutter and workpiece are separated.

So, to expound the separation condition of intermittent high-frequency intermittent contact caused by supersonic vibration better, the velocity coefficient P is introduced as Eq. (5) [18].

$$P = \frac{V_z \sin\beta}{V_c \cos\beta}. \quad (5)$$

In combination with the above analysis results, the cutter has the following separation conditions for intermittent cutting in the ultrasonic milling processing based on the theoretical analysis: ① The processing cutter for supersonic vibration is at the workpiece separation stage when $P > 1$; ② The processing cutter for supersonic vibration is at the critical value of the workpiece separation state when $P = 1$; ③ The processing cutter for supersonic vibration is at the workpiece contact stage when $P < 1$.

2.2 Auxiliary Milling Mechanism of Axial Supersonic Vibration

Auxiliary milling device of supersonic vibration mainly includes the ultrasonic power supply, energy converter, ultrasonic handle, and milling cutter. When a supersonic vibration system starts operation, firstly, the ultrasonic power supply sends out a current signal and delivers it to the energy converter, then the energy converter converts the current signal to the sine pulse signal. Finally the power amplifier in the ultrasonic handle amplifies the vibration amplitude and outputs the vibration information matched with energy converter through the cutter, namely the supersonic vibration auxiliary milling, as shown in Figure 2.

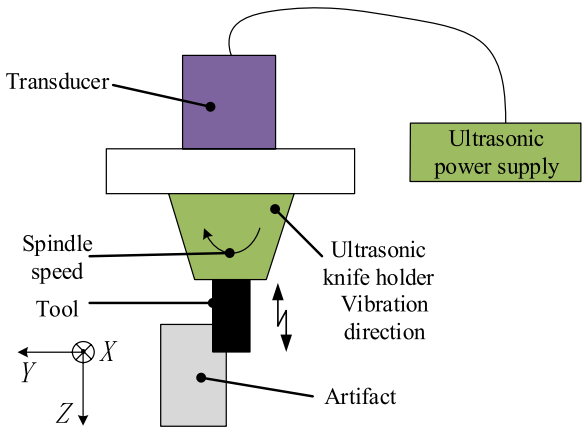

Figure 2 Schematic diagram of auxiliary milling system of axial supersonic vibration

Table 1 Experiment parameters for verification of surface roughness empirical model

Serial number	Spindle speed (r/min)	Feed per tooth (mm/z)	Depth of cut (mm)
1	900	0.08	6
2	1600	0.09	6
3	1700	0.06	9
4	1800	0.07	4

2.3 Establishment of 3D Milling Simulation Model

The milling simulation through finite element software is relatively macro due to less surface roughness value, so the tiny element simulation is conducted to the milling, and the 3D bevel cutting simulation replaces the 3D milling simulation for the research on surface roughness. The surface roughness is the mean value of tiny displacement variation for contour on the surface of the cutting processing workpiece in essence. Since the finite element software doesn't have the module for direct measurement of surface roughness, the simulation measurement could be conducted to the infinitesimal displacement variation of contour on the surface of the processed workpiece as the parameters for predicting the surface roughness value. The specific milling parameters are shown in Table 1.

2.3.1 Constitutive Model of Materials

The J-C constitutive model proposed by Jonson et al. is widely applied in the metal cutting field, so the J-C constitutive model is adopted upon the establishment of the

titanium alloy milling finite element simulation model, which considers the axial supersonic vibration, as shown in Eq. (6).

$$\sigma = \left[A + B(\varepsilon)^n\right] \cdot \left[1 + C \ln \frac{\dot{\varepsilon}}{\dot{\varepsilon}_0}\right] \cdot \left[1 - \left(\frac{T - T_r}{T_m - T_r}\right)^m\right], \tag{6}$$

where σ is equivalent flow stress (MPa); ε is equivalent plastic strain rate; ε_0 is the reference plastic strain rate. T is the absolute temperature of the workpiece material ($\dot{\varepsilon}_0 = 0.001\text{s}^{-1}$); T_r is room temperature ($T_r = 25$ ℃); T_m is melting temperature; A is yield strength; B is the hardening modulus; C is strain rate sensitivity coefficient; m is thermal softening coefficient; n is the strain hardening index [19].

2.3.2 Material Failure Criteria

In the milling processing process, as the rack face constantly extrudes the materials, the materials are continuously removed to form different shapes of chips. The damage coefficient is deemed as an essential parameter that can judge whether materials are invalid in the failure criterion of Johnson-Cook, and is indicated with D (materials are considered to be weak when D is more than 1) in general [20], with the calculation equation as Eq. (7).

$$D = \sum \frac{\Delta \bar{\varepsilon}^{pl}}{\bar{\varepsilon}_f^{pl}}, \tag{7}$$

where $\Delta \bar{\varepsilon}^{pl}$ and $\bar{\varepsilon}_f^{pl}$ refer to the equivalent plastic strain increments and the equivalent plastic strain upon unit failure, respectively. Its expression equation is shown in Eq. (8):

$$\bar{\varepsilon}_f^{pl} = [d_1 + d_2 \text{epx}(-d_3)\eta]\left[1 + d_4 \ln(\frac{\bar{\varepsilon}^{pl}}{\bar{\varepsilon}_0})\right](1 - d_5\theta), \tag{8}$$

where $\bar{\varepsilon}_0$ refers to the reference strain rate; $\bar{\varepsilon}$ refers to the plastic strain rate; d_1, d_2, d_3, d_4, d_5 refers to the material failure parameters.

2.3.3 Chips Contact Model

By the friction model [21] proposed by Zorev, the contact segment between the cutter and cutting layer area is divided into the bonded area and slipping place in the established simulation model. In the slipping area, the friction coefficient is a constant, and its change scope meets the Coulomb Friction Law, as shown in Eq. (9).

$$\tau = \begin{cases} \mu\sigma_n & 0 < x < l_p, \\ \tau_p & l_p < x < l_c, \end{cases} \tag{9}$$

where σ_n refers to the normal stress; τ_p and μ refer to shear stress and friction coefficient, respectively.

2.3.4 Setting of Ultrasonic Motion Trial of Shank Cutter

In the established axial supersonic vibration auxiliary milling 3D model, the feeding direction of milling isn't fixed, and the centrode of the cutter is a regular wavy curve. In ABAQUS software, the load function module can control the amplitude value curve by setting up boundary conditions or load with the change of time and frequency, thus achieving the simulation condition of a non-linear cutter centrode.

The same-cycle amplitude curve is adopted in the model to control the motion mode of the cutter, which is calculated in the amplitude equation in the setting of the parameter process, in which the amplitude's circular frequency has the following calculation equation:

$$\omega = 2\pi f \text{t}, \tag{10}$$

where ω, f and t refer to the circular frequency, the vibration frequency of the cutter, and the period, respectively. The cutter's vibration frequency and time span are 25 kHz and 0.1 s, respectively.

In the amplitude value parameter setting module, in addition to setting up the circular frequency, the size of vibration amplitude shall be set, namely the setup of parameters A and B, whose specific relationship as below:

$$u = A_0 + A\cos 2\pi f + B\sin 2\pi f, \tag{11}$$

where u and A_0 refer to the amplitude and the initial amplitude, respectively; A and B refer to amplitude control parameters.

The vibration amplitude needs to be set as 10 μm. So if we put the control parameter A of initial amplitude and amplitude as 0, the value of B is equal to the amplitude value. The specific parameter setting of amplitude value could be found at Figures 3 and 4.

2.4 Post-treatment of Finite Simulation Model

The arithmetic average deviation Ra of contour refers to the arithmetic average of surface contour offset absolute value of manufacturing workpiece in the sampling length l, and can accurately and comprehensively reflect the microscopic unevenness of surface [22], as shown in Figure 5, with expression equation as below:

$$Ra = \frac{1}{n}\sum |y_i|, \tag{12}$$

wherein, y_i refers to the distance between the point and center line on contour.

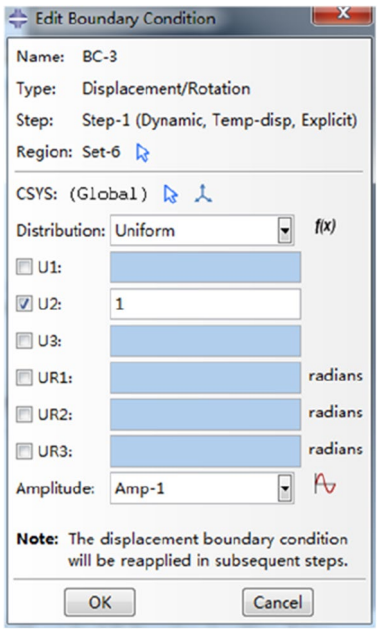

Figure 3 Load setting in ABAQUS software

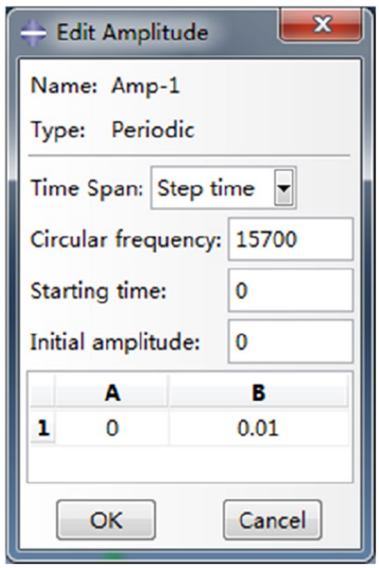

Figure 4 Setting of vibration amplitude curve parameters

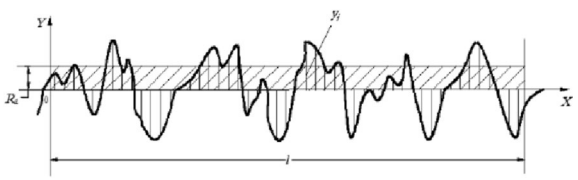

Figure 5 Diagram of arithmetic average deviation [23]

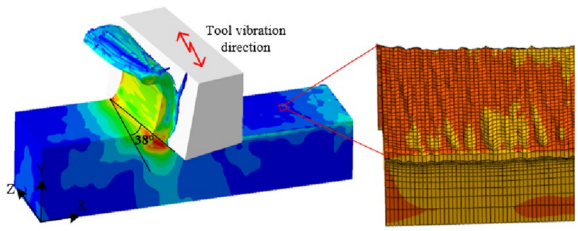

Figure 6 Imitated diagram of workpiece surface roughness

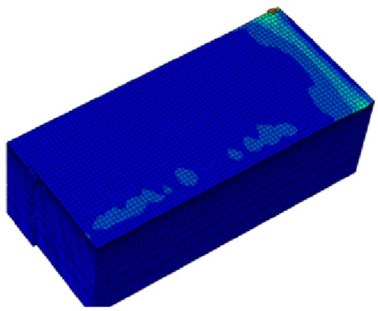

Figure 7 Simulation result graph after concealment of cutter and chips

Figure 6 is the imitated diagram of surface roughness after simulation processing. When the surface roughness model is predicted through finite element simulation, the infinitesimal element processing is conducted to the auxiliary milling of supersonic vibration, which is replaced with bevel chips.

To facilitate the research on the simulation result graph of surface roughness, the cutter and chips are hidden, as shown in Figure 7.

The bevel cutting simulation is conducted on the workpiece. The grid node is selected on the surface of the workpiece and is magnified to the maximum degree, and any point around it is set. The mean value between the workpiece radial coordinate values (coordinate value Y) of extraction point in the actual cutting process and the absolute value of theoretical difference value of workpiece radial coordinate values is deemed to be the workpiece's processing surface contour height Ra. The field output module selects the displacement field output to extract the surface roughness value. Twenty-one points on the processed surface after the stable cutting of the workpiece are chosen. The absolute value of the 21 groups of the extracted surface roughness parameters is calculated, as shown in Figure 8.

The specific value of cutting parameters in Group 2 of Table 1 is shown in Table 2. Finally, the absolute value

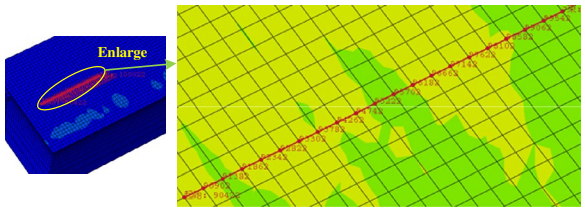

Figure 8 Coordinate extraction figure

Table 2 Extraction data of surface roughness

Serial number	y_i (μm)	Absolute value of y_i (μm)
1	0.9886	0.989
2	0.8354	0.835
3	0.145	0.145
4	0.552	0.552
5	0.6107	0.611
6	0.6417	0.642
7	0.7232	0.723
8	0.401	0.401
9	0.46	0.46
10	0.6516	0.652
11	0.224	0.224
12	0.1885	0.189
13	0.435	0.435
14	0.55	0.55
15	0.6506	0.651
16	0.647	0.647
17	0.479	0.479
18	0.512	0.512
19	0.1057	0.106
20	0.1678	0.168
21	0.216	0.216

Table 3 Surface roughness value obtained through finite element simulation

Serial number	Spindle speed (r/min)	Feed per tooth (mm/z)	Depth of cut (mm)	*Ra* (μm)
1	900	0.08	6	0.327
2	1600	0.09	6	0.509
3	1700	0.06	9	0.346
4	1800	0.07	4	0.314

of y_i in Table 2 is analyzed based on Eq. (12), and the surface roughness *Ra* is 0.509.

Likewise, the simulation results of milling parameters in Table are processed to work out the surface roughness of each group of processing parameters, as shown in Table 3.

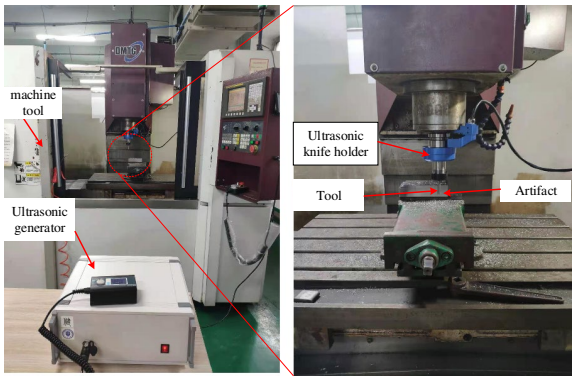

Figure 9 Test Platform in this research

Table 4 Cutter parameters

Parameter	Parameter value (°)
Helix angle	38
Front angle	8
Back angle	9
Interdental angle	90

3 Empirical Model of Surface Roughness Based on ANOVA

3.1 Construction of Test Platform

The equipment used in the experiment can be divided into the processing center, supersonic vibration system, and workpiece. As shown in Figure 9, the experimental machine tool adopts the VDL-1000E three-axis milling machine, the workpiece materials adopt titanium alloy, the ultrasonic power frequency is 25 kHz, and the cutter adopts the 4-blade ϕ10 cemented carbide flat milling cutter, with the specific parameters shown in Table 4. The workpiece connects its machine tool workbench, and the ultrasonic handle connects the main shaft.

3.2 Orthogonal Test Design and Specific Test Parameters

The test study adopts the orthogonal test method, which is a kind of commonly-used research method of inquiring about the multi-factor variables at present. The orthogonal test can reduce test times as far as possible, rapidly obtain the representative test data, improve the test progress and guarantee the reliability of test results. The specific test parameters are shown in Table 5.

Table 5 Multi-factorial test parameter table

Vibration frequency (kHz)	25	Amplitude (μm)	8
Factor	Level		
	I	II	III
A- Spindle speed (r/min)	1000	1500	2000
B- Feed per tooth (mm/z)	0.05	0.07	0.09
C- Depth of cut (mm)	3	6	9

The test aims to research the surface roughness, the multi-factorial test, which involves four factors and three levels and considers the mutual influence among each aspect, is designed. The header design of the test scheme is shown in Table 6.

3.3 Test Results and Analysis of Surface Roughness Based on ANOVA

The single-factor analysis results of workpiece surface roughness in the last section show that the rotation speed and feed speed of the main shaft are the leading causes of influencing the surface roughness of the processed workpiece. But in the actual milling process, their influence on the surface roughness of the workpiece is mutually influenced. Based on that issue, the response surface methodology will analyze the impact of interaction among three cutting factors on surface roughness to seek the optimal milling parameter combination. The test result is shown in Table 7.

3.4 Surface Roughness Modeling Based on RSM

The variance method is adopted to analyze the rule of influence of milling parameters on the surface roughness of the processed workpiece. Still, the interaction among each milling parameter in actual cutting processing is excellent. Hence, response surface methodology shall be utilized to analyze the optimization results further. Response surface methodology (RSM) is a method to optimize statistical trials of random processes. It has the functions of test design, regression analysis, interaction

Table 6 Multi-factor header design

Factor	*A*	*B*	(*A***B*)1	(*A***B*)2	*C*	(*A***C*)1	(*A***C*)2	(*B***C*)1	(*B***C*)2
No.	1	2	3	4	5	6	7	8	9

Table 7 Experimental result

No.	*A*	*B*	(*A***B*)1	(*A***B*)2	*C*	(*A***C*)1	(*A***C*)2	(*B***C*)1	(*B***C*)2	Ra
1	I	I	I	I	I	I	I	I	I	0.275
2	I	I	I	I	II	II	II	II	II	0.326
3	I	I	I	I	III	III	III	III	III	0.403
4	I	II	II	II	I	I	I	II	III	0.553
5	I	II	II	II	II	II	II	III	I	0.564
6	I	II	II	II	III	III	III	I	II	0.864
7	I	III	III	III	I	I	I	III	II	1.130
8	I	III	III	III	II	II	II	I	III	1.231
9	I	III	III	III	III	III	III	II	I	1.310
10	II	I	II	III	I	II	III	I	I	0.225
11	II	I	II	III	II	III	I	II	II	0.255
12	II	I	II	III	III	I	II	III	III	0.317
13	II	II	III	I	I	II	III	II	III	0.374
14	II	II	III	I	II	III	I	III	I	0.420
15	II	II	III	I	III	I	II	I	II	0.452
16	II	III	I	II	I	II	III	III	II	0.742
17	II	III	I	II	II	III	I	I	III	0.745
18	II	III	I	II	III	I	II	II	I	0.957
19	III	I	III	II	I	III	II	I	I	0.234
20	III	I	III	II	II	I	III	II	II	0.300
21	III	I	III	II	III	II	I	III	III	0.321

analysis, etc. Such analysis method considers the interaction effect and secondary effect among every process parameter, with the expression eqution as follows:

$$Y = Ra - \varepsilon = \beta_0 + \sum_{i}^{k} \beta_i x_i + \sum_{i=1}^{k-1} \sum_{j=i+1}^{k} \beta_{ij} x_i x + \sum_{i=1}^{k} \beta_{ij} x_i^2, \tag{13}$$

where Y refers to the response value of surface roughness, x_i and x_j refer to the independent variable, Ra refers to the surface roughness; β_0, β_{i}, β_{ij} and β_{ii} refer to the regression coefficient of each item.

Based on the Design-Expert 8.0.6 software, the stepwise regression analysis method is utilized for the repeated optimization processing of test data in Table 7 to process the platform. The stepwise regression analysis is conducted to the test data in Table 7 through Design-Expert 8.0.6 software, and the repeated consequent selection and reverse removal are completed to the test data to work out the Level-II response surface analysis model equation of titanium alloy surface roughness based on three cutting factors:

$$\begin{aligned} Ra =& 0.49 - 0.15A + 0.32B \\ &+ 0.088C - 0.082A * B \\ &- 0.064A * C + 0.027B * C \\ &+ 0.14A^2 + 0.046B^2 + 0.025C^2, \end{aligned} \tag{14}$$

Table 8 Significance analysis of surface roughness regression model

Source of variance	Sum of square	Degree of freedom	Mean square	*F* value	*P*-value
A	0.17	1	0.17	41.84	0.0009
B	0.84	1	0.84	208.97	≤ 0.0001
C	0.059	1	0.059	14.86	0.0130
AB	0.028	1	0.028	7.01	0.0331
AC	0.017	1	0.017	4.12	0.0818
BC	0.003042	1	3.042×10^{-3}	0.76	0.4790
A^2	0.057	1	0.057	14.30	0.0071
B^2	1.980×10^{-3}	1	1.980×10^{-3}	0.49	0.353
C^2	1.698×10^{-3}	1	1.698×10^{-3}	0.042	0.5100

where A, B and C refer to the rotation speed of the main shaft, feed speed and cutting depth, respectively.

3.5 Optimization and Inspection of Surface Roughness Regression Model

To improve the accuracy of the established regression model of surface roughness, the Design-Expert 8.0.6 software is adopted for significance analysis of all independent variables in the model. If the value P of the tested objects among analysis results is no more than 0.05, such thing is significant. Otherwise it is non-significant.

As shown in Table 8, B of the primary item is highly significant, $A2$ of direct item, the interaction item, and the quadratic term are substantial, and $B2$ and $C2$ of the interaction item and the quadratic term are not significant.

To obtain the optimal surface roughness model, the optimal principle of the regression equation is utilized to eliminate the non-significant value in the significant analysis module and optimize the established model. The response surface analysis model of titanium alloy surface roughness is:

$$\begin{aligned} Ra =& 0.49 - 0.15A + 0.32B + 0.088C \\ &- 0.082A * B + 0.14A^2. \end{aligned} \tag{15}$$

To verify the accuracy of the optimized model, a significance analysis is needed for the model to judge the reliability of the model, as shown in Table 9.

3.6 Optimization of Auxiliary Milling Auxiliary Titanium Alloy Process Parameters for Supersonic Vibration

The visual processing analysis is conducted to the optimized surface roughness regression model through Design-Expert 8.0.6 software. Based on the fixed parameter, the rule of influence of interaction between any two milling parameters on titanium alloy surface roughness is shown; the optimal value of surface roughness is $Ra = 0.277$ μm, and the corresponding milling process parameters $A = 1403.29$ r/min, $B = 319.75$ mm/min, $C = 3.1$ mm, as shown in Figure 10.

As shown in Figure 10, the surface roughness changes a little with the increase in rotation speed of the main

Table 9 Significance verification of surface roughness regression model

Source of variance	Sum of square	Degree of freedom	Mean square	*F* value	*P* value
Regression model	1.27	9	0.14	25.99	≤ 0.0001
Residual	0.038	7	5.441×10^{-3}		
Lack of fit	0.024	3	8.100×10^{-3}	2.35	0.2137
Pure error	0.014	4	3.447×10^{-3}		
Sum	1.31	16			

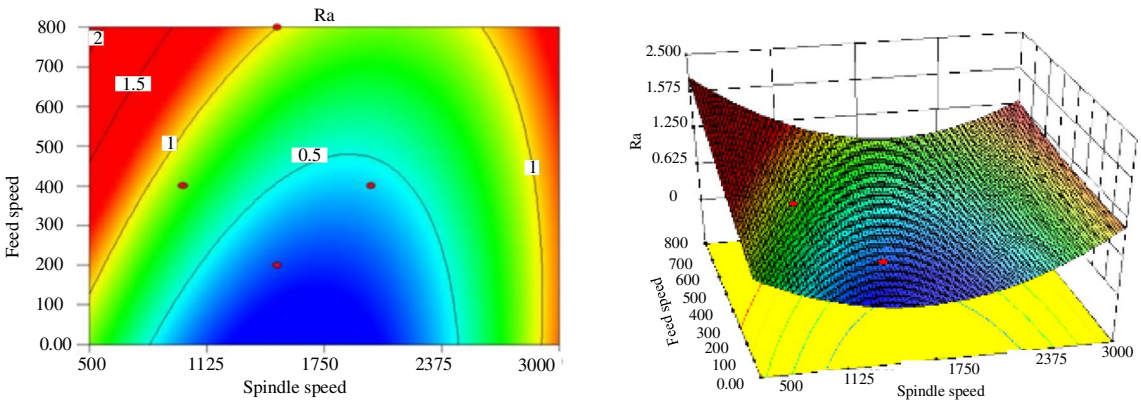

Figure 10 3D response surface figure of surface roughness regression equation [response surface and contour of (*A*) and (*B*)]x

shaft; surface roughness would rapidly increase with the addition in feed rate of every gear. The feed rate of every equipment becomes the most critical factor in influencing the surface roughness of the workpiece, because the remaining height of the processing surface is mainly controlled by the tool nose's radius and feed rate. When the radius of the tool nose is fixed, the remaining size of the processing surface will increase with the increase of the feed rate of every gear.

As shown in Figure 11, the surface roughness value changes a little with the increase of cutting depth, and the surface roughness decreases before increasing with the growth in rotation speed of the main shaft. The surface roughness reduces mainly because the increase of rotation speed of main shaft improves the contact rate between cutter and workpiece and reduces the surface roughness *Ra*; later, with the promotion of rotation speed of the main shaft, the strengths of vibration milling reduce, and secondary "ironing" becomes poor, causing the surface roughness becomes poor.

As shown in Figure 12, with the increase of the feed rate of every gear, the growth trend of surface roughness isn't apparent, which indicates that the interaction between the feed rate of every equipment and the cutting depth doesn't generate a significant influence on surface roughness.

3.7 Experimental Verification of Regression Model and Optimal Milling Parameters

To verify whether the milling parameter corresponding to the optimal value of workpiece surface roughness through model analysis is accurate, the optimal combination of supersonic vibration milling process parameters is adopted for the milling process of titanium alloy. The number of terms and the times of independent variables contained in the surface roughness empirical model can be adjusted sharply. The model precision can be improved by increasing the number of high-order terms [21]. So, the established surface roughness empirical model has made good progress.

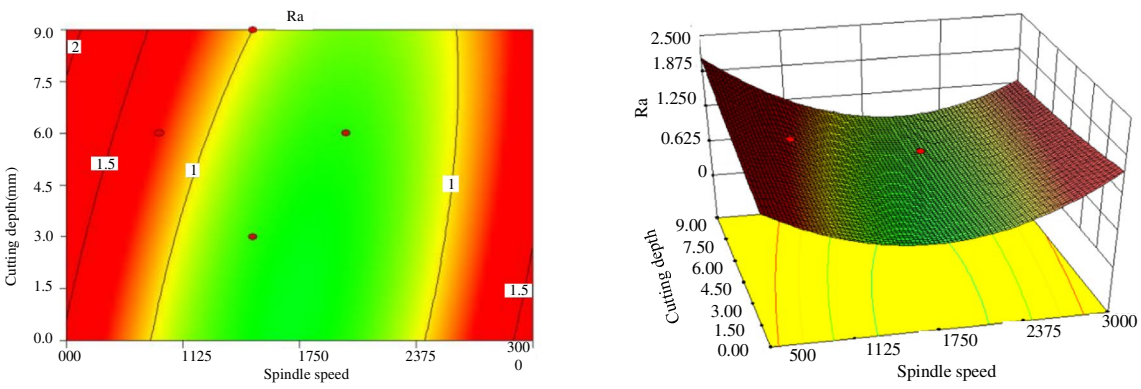

Figure 11 3D response surface figure of surface roughness regression equation [response surface and contour of (*A*) and (*C*)]

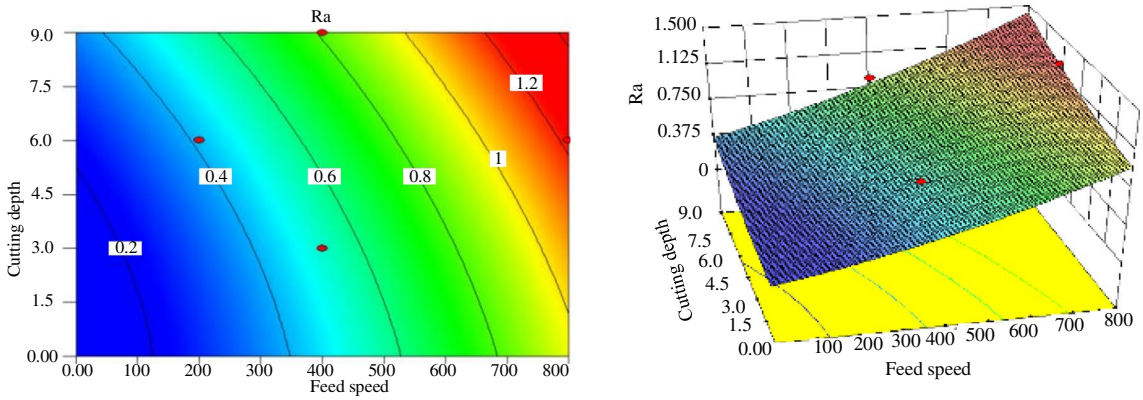

Figure 12 3D response surface figure of surface roughness regression equation [response surface and contour of (B) and (C)]

Table 10 Comparison between experimental result and simulation result

Serial number	RSM model prediction result (μm)	FEM simulation result (μm)	Experimental result (μm)
1	0.432	0.327	0.451
2	0.686	0.509	0.726
3	0.430	0.346	0.483
4	0.423	0.314	0.455

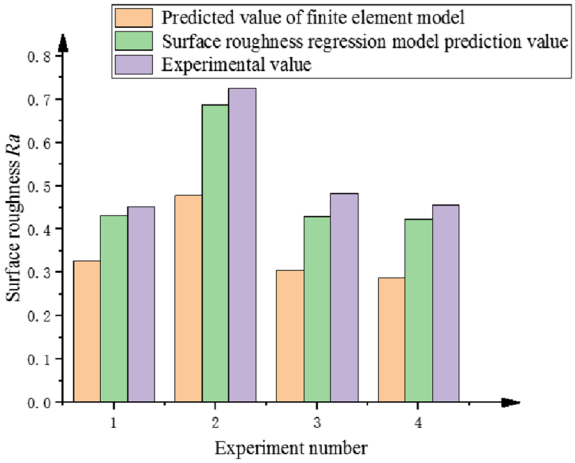

Figure 13 Comparison Diagram of Surface Roughness

The finite element simulation model and surface roughness prediction model are verified and analyzed by experiment. The comparison result can be found in Table 10.

As shown in Figure 13, the predicted error range of the surface roughness model of the workpiece and the finite element simulation model is 4.4%–12.3% and 27.5%–30.9%, respectively, and the surface roughness empirical model has higher fitting precision. The comparison results between the predicted value and the experiment value show that experiment value is more significant than the predicted value, and the error is mainly generated due to the following causes:

(1) **For simulation research** For the simulation process is ideal, the inevitable external factors such as the vibration of the machine tool and the clamping error between tool and workpiece in the actual machining process are not considered. In the ultrasonic vibration-assisted machining process, the amplitude is minimal. Slight vibration may have a relatively significant impact on the experimental results, and there are measurement errors in the experiment. Also, for the process of FEM simulation, with the continuous cutting of the tool, the mesh elements on the workpiece will be distorted, which will also affect the simulation results.

(2) **For empirical model research** On the one hand, the influence of tool wear on surface roughness was not considered in the test process. On the other hand, due to the vibration of the machine tool in the machining process and the inherent processing characteristics of the material, making the model prediction has an error. In ultrasonic vibration milling, the fracture of the chip and the forming mechanism of the machined surface have changed dramatically due to the introduction of axial vibration. Due to the action of ultrasound, the cutting edge of the tool is intermittently separated from the workpiece in high frequency and cycle, which makes the

cutting edge have a reciprocating "ironing" effect on the machined surface, so there is deviation compared to the actual measurement process.

4 Conclusions

The auxiliary milling surface roughness of axial supersonic vibration is researched by simulation and experimental methods. The conclusions are as follows:

(1) The finite element software is used to simulate the micro displacement variation of the machined workpiece surface contour. The surface roughness obtained by the finite element simulation model is verified by experiments, and the error range is 27.5%–30.9%. The empirical model of surface roughness obtained by the response surface method is verified by experiments, and the error is between 4.4% and 12.3%.

(2) Under the premise of not considering the influence of cutter abrasion on the surface roughness, the predicted value of the surface roughness empirical model obtained in the test method is more accurate than that of surface roughness by finite element simulation, mainly because the processing environment of finite element simulation is relatively ideal. The test method is more suitable for the actual process in comparison to the finite element simulation method.

Acknowledgements
Not applicable.

Author contributions
XW and CY were in charge of the trial; XW and CY wrote the manuscript; DH and XL assisted with sampling and laboratory analyses. All authors read and approved the final manuscript.

Authors' Information
Xuetao Wei born in 1995, is currently a master candidate at *Key Laboratory of Advanced Manufacturing and Intelligent Technology, Ministry of Education, Harbin University of Science and Technology*, *China*. He received his bachelor degree from *Harbin University of Science and Technology, China*, in 2018. His research interest is ultrasonic vibration aided machining.
E-mail: 759361080@qq.com
Caixu Yue born in 1982, is currently a professor at *Harbin University of Science and Technology, China*. He received his Ph.D. degree from *Harbin University of Science and Technology, China*, in 2012. His research interest is digital processing technology.
E-mail: yuecaixu@hrbust.edu.cn
Desheng Hu born in 1996, is currently a master candidate at *Key Laboratory of Advanced Manufacturing and Intelligent Technology, Ministry of Education, Harbin University of Science and Technology*, *China*.
E-mail: 1286677393@qq.com
Xianli Liu born in 1961, is currently a professor at *Harbin University of Science and Technology, China*. His research interest is intelligent manufacturing technology.
E-mail: xlliu@hrbust.edu.cn
Yunpeng Ding born in 1988, is currently a lecturer at *Suzhou Vocational Institute of Industrial Technology, China*. His research interest is digital precision machining and monitoring.
E-mail: dyp_122@163.com
Steven Y. Liang born in 1958, is currently a professor at *George W. Woodruff School of Mechanical Engineering, Georgia Institute of Technology, US*. His research interests include intelligent manufacturing and ultra precision machining technology.
E-mail: steven.liang@me.gatech.edu

Funding
Supported by National Natural Science Foundation of China (Grant No. 52175393).

Competing interests
The authors declare no competing financial interests.

Author Details
[1]Key Laboratory of Advanced Manufacturing and Intelligent Technology, Ministry of Education, Harbin 150080, China. [2]Department of Precision Manufacturing Engineering, Suzhou Vocational Institute of Industrial Technology, Suzhou 215104, China. [3]George W. Woodruff School of Mechanical Engineering, Georgia Institute of Technology, Atlanta 30332, USA.

Received: 17 July 2021 Revised: 8 May 2022 Accepted: 14 June 2022
Published online: 03 August 2022

References

[1] D Biermann, P Kersting, T Surman. A general approach to simulating work- piece vibrations during five-axis milling of turbine blades. *CIRP Annals. Manufacturing Technology*, 2010, 59: 125-128.
[2] J J Wang, C L Zhang, P F Feng, et al. A model for prediction of subsurface damage in rotary ultrasonic face milling of optical K9 glass. *The International Journal of Advanced Manufacturing Technology*, 2016, 83: 1-4.
[3] X H Shen, J H Zhang, Xing D L. Ultrasonic vibration milling kinematics and its influence on cutting force. *Journal of Shenyang University of Technology*, 2012, 34(5): 530-535.
[4] Alfredo Suárez, Fernando Veiga, Luis N, et al. Effects of ultrasonics-assisted face milling on surface integrity and fatigue life of Ni-Alloy 718. *Springer US*, 2016, 25: 5076-5086.
[5] François Ducobu, Pedro-José Arrazola, Edouard Rivière-Lorphèvre. Finite element prediction of the tool wear influence in Ti6Al4V machining. *Procedia CIRP*, 2015, 31: 124-129.
[6] Y Yang, Y L Ke, H Y Dong. Constitutive model of aviation aluminum alloy sheet in metal cutting. *Chinese Journal of Nonferrous Metals*, 2005, 06: 854-859.
[7] Z G Huang, Y L Ke, L T Wang. Research on thermo-mechanical coupling model and finite element simulation of metal cutting. *Journal of Aeronautics*, 2004, 3: 317-320.
[8] H Y Dong. *Numerical simulation of the machining process of aviation integral structural parts*. Hangzhou: Zhejiang University, 2004.
[9] J Sun. *Research on the theory and method of deformation correction in numerical control machining of aerospace integral structure*. Hangzhou: Zhejiang University, 2003.
[10] G B Li. *Finite element simulation experiment research on micro metal cutting process*. Tianjin: Tianjin University, 2010.
[11] Moaz H Ali, Basim A Khidhir, M N M Ansari. FEM to predict the effect of feed rate on surface roughness with cutting force during face milling of titanium alloy. *HBRC Journal*, 2013, 9: 263-269.
[12] Thanongsak Thepsonthi,Tuğrul Özel. 3-D finite element process simulation of micro-end milling Ti-6Al-4V titanium alloy: Experimental validations on chip flow and tool wear. *Journal of Materials Processing Tech.*, 2015, 221: 128-145.
[13] Riaz Muhammad, Naseer Ahmed, Murat Demiral, et al. Computational study of ultrasonically-assisted turning of Ti alloys. *Advanced Materials Research*, 2011, 1243: 30-36.

[14] Sandip Patil, Shashikant Joshi, Asim Tewari, et al. Modelling and simulation of effect of ultrasonic vibrations on machining of Ti6Al4V. *Ultrasonics*, 2014, 54(2): 694-705.
[15] Y H Chun, C H Huang. A Study on ultrasonic vibration milling of inconel 718. *Key Engineering Materials*, 2010, 854(9):169-172.
[16] Z Abootorabi, M R Razfar, A Abdullah. Influence of ultrasonic vibrations on side milling of AISI 420 stainless steel. *The International Journal of Advanced Manufacturing Technology*, 2013, 66: 1-4.
[17] Junichiro Kumabe. *Precision machining vibration cutting* (*basic and application*). Beijing: Mechanical Industry Press, 1985.
[18] X W Wang. *Research on milling mechanism and surface quality of SiCp/AL under ultrasonic excitation*. Taiyuan: North University of China, 2018.
[19] M M Wang. *Experimental research on high temperature dynamic mechanical properties of Ti-5553 and its matching with tool materials*. Harbin: Harbin University of Science and Technology, 2018.
[20] Y W Wang. Tool optimization for hard milling of spliced die based on finite element simulation. Harbin: Harbin University of Science and Technology, 2019.
[21] N N Zorev. Inter-relationship between shear processes occurring along tool face and on shear plane in metal cutting. *International Research in Production Engineering*. New York: ASME,1963:42-49.
[22] Q Wu. Research on cutting force and surface roughness of high-speed turning 45# Steel in cutting stability region. Lanzhou: Lanzhou University of Technology, 2020.
[23] B L Li. Polynomial regression and local regression methods. *Journal of Jinan University (Natural Science and Medicine Edition)*, 2003, 3: 6-9.